Peer-reviewed version available at Water 2019, 11, 248; doi:10.3390/w11020248

Evaluation of Fengyun-3C Soil Moisture Products Using In situ Data from the Chinese Automatic Soil Moisture Observation Stations: A Case Study in Henan Province, China

Yongchao Zhu[1,2], Simon Pearson[3], Dongli Wu[4], Ruijing Sun[5], Shibo Fang[1,2]*

[1] State Key Laboratory of Severe Weather, Chinese Academy of Meteorological Sciences, Beijing, 100081, China; ychzhuvip@yeah.net;
[2] Collaborative Innovation Centre on Forecast and Evaluation of Meteorological Disasters, Nanjing University of Information Science & Technology, Nanjing, 210044, China;
[3] Lincoln Institute for Agri-Food Technology, University of Lincoln, Lincoln, LN67TS, United of Kingdom; SPearson@lincoln.ac.uk;
[4] Chinese Meteorological Observation Centre, Meteorological Administration Meteorological, Beijing, 100081, China; wudongli@cma.gov.cn;
[5] National Satellite Meteorological Centre, China Meteorological Administration, Beijing, 100081, China; sunrj@cma.gov.cn.
* Correspondence: fangshibo@cma.gov.cn; Tel.: +86-15801635580

Abstract: Soil moisture (SM) products derived from passive satellite missions are playing an increasingly important role in agricultural applications, especially in crop monitoring and disaster warning. Evaluating the dependability of those products before they can be used on a large scale is crucial. In this study, we assessed the level 2 (L2) SM product from the Chinese Fengyun-3C (FY-3C) radiometer against in situ measurements collected from the Chinese Automatic Soil Moisture Observation Stations (CASMOS) during a one-year period from January 1 to December 31, 2016 in Henan, which is an agricultural province in China. Four statistical parameters were used to evaluate the products' reliability: mean difference, root-mean-square error (RMSE), unbiased RMSE (ubRMSE), and the correlation coefficient. These statistical indicators revealed that the FY-3C L2 SM product generally did not agree with the in situ SM data from CASMOS. The time-series analysis further indicated that the correlations and estimated error were highly related to the growing periods of the crops in our study area. FY-3C L2 SM data tended to overestimate soil moisture during May, August, and September, when the crops reach their maximum vegetation density, and tended to underestimate the soil moisture content during the rest of the year. The averaged correlation coefficient between FY-3C SM and the Moderate Resolution Imaging Spectroradiometer (MODIS) normalized difference vegetation index was 0.55, which demonstrates that the vegetation water content of the crops considerably influences the SM product. To improve the accuracy of the FY-3C SM product, an improved algorithm that can filter out the influences of the crops should be applied in the future.

Keywords: Soil moisture; Fengyun-3C; Passive microwave; Chinese Automatic Soil Moisture Observation Stations; NDVI

1. Introduction

Soil moisture (SM) is one of the fundamental environmental variables in the global energy and water cycles [1]. As satellite-based soil moisture products have become more widely available, they have played increasingly important roles in many applications, such as meteorology, hydrology, climatology, and agriculture [2]. Accurate measurement of soil moisture on large scales may assist in crop yield estimation, drought prediction, and disaster monitoring in agricultural regions,

particularly in arid and semiarid regions where regular irrigation is required but water resources are limited.

Soil moisture soil surface information can be obtained by various means, such as in situ soil moisture instruments, land surface models, and remote sensing technology [3]. Since the first passive microwave satellite sensor was launched in 1978, various studies have demonstrated that it is feasible to retrieve soil moisture from passive microwave satellite missions [4]. Many passive microwave satellite missions have been widely used for soil moisture estimation, such as the Soil Moisture and Ocean Salinity (SMOS) mission [5,6], the Soil Moisture Active/Passive (SMAP) mission [7], the Special Sensor Microwave/Imager (SSM/I) mission, the Advanced Microwave Scanning Radiometer for the Earth Observing System (AMSR-E) [8,9], the Advanced Microwave Scanning Radiometer 2 (AMSR2) mission [10], and a series of China's Fengyun 3 (FY-3) satellites, consisting of FY-3A, FY-3B, FY-3C, and FY-3D [11-13].

Since soil moisture products are generally based on different satellite data and algorithms, their quality and continuity vary in space and time [14]. Validation is an important task for any satellite-based soil moisture product, as it not only aids in appraising the actual accuracy of the delivered soil moisture estimates but also improves our understanding of the product's advantages and disadvantages under different ground conditions and at different times [15]. Numerous studies have assessed the accuracy of the soil moisture products from SMOS, SMAP, AMSR-E, and AMSR2 by comparing the estimations against the ground measurements from monitoring networks around the world [2,3,5,16-21]. However, to the best of our knowledge, limited research has focused on evaluating the accuracy of the soil moisture product from FY-3 series satellites, particularly over agricultural areas.

FY-3C, as the third satellite in the FY-3 series, was launched on September 23, 2013. A microwave radiation imager (MWRI) was aboard this satellite, which observes the Earth's surface at five different microwave frequencies ranging from 10 to 89 GHz. The FY-3C MWRI can complete the coverage of the Earth's surface within two to three days, with a swath of 1400 km. Local crossing times are around 10:00 p.m. and 10:00 a.m. for ascending and descending overpasses, respectively [22]. Observations from the FY-3C MWRI have been used to retrieve the land surface parameters such as soil moisture, vegetation water content, and land surface temperature.

An official soil moisture product derived from the MWRI observations was distributed by the National Satellite Meteorological Centre (NSMC) of China, which is available for all registered users. To obtain the official soil moisture product from the MWRI observed brightness temperatures, NSMC used a modified version of a soil moisture retrieval algorithm originally developed by Njoku et al. [9]. The National Aeronautics and Space Administration (NASA) first adopted the algorithm as their official soil moisture retrieval algorithm for observations of the AMSR-E sensor, in which the brightness temperatures of 10.7 and 18.7 GHz were used to retrieve soil moisture using an iterative inversion algorithm. Since the FY-3C MWRI configuration is almost identical to that of AMSR-E, it is expected to sense and record soil moisture content contained in the top ~1 cm of the soil layer, on average, for low-vegetated areas [3,23]. Several studies evaluated this retrieved algorithm by comparing it with soil moisture products from other retrieval algorithms and ground-based measurements [13,24-26]. These preceding analyses suggest that the best agreement with in situ measurements was found in sparsely- to moderately-vegetated regions and that agreement would decrease with increasing vegetation density.

In this paper, we aimed to evaluate the level 2 (L2) soil moisture product from FY-3C MWRI over agricultural regions. Henan province, an agricultural region in China where the crop rotation consists mainly of winter wheat and summer maize, was chosen as our study area. To assess the performance of the FY-3C L2 SM data over this agricultural region, we compared the product with in situ soil moisture data from 144 monitoring stations from the Chinese Automatic Soil Moisture Observation Stations (CASMOS) Network over a one-year period from January 1 to December 31, 2016 at daily and monthly time scales in Henan province. We evaluated the soil moisture product using four statistical parameters: the mean difference (MD), the root-mean-square error (RMSE), the

unbiased RMSE (ubRMSE), and the correlation coefficient (*R*). Additionally, we analyzed how the cropping system affected the FY-3C soil moisture product performance over the region.

2. Study area and Datasets

2.1. Study Area

Henan province, located in the middle part of China (Figure 1b), is one of the most important granaries in the country, extending from 31°23′ N to 36°22′ N and 110°21′ E to 116°39′ E, with an area of 16.7 × 104 km² and an average elevation of 100 m above sea level. Henan has a typical temperate monsoon climate and an annual mean temperature of 10–15 °C. The annual precipitation is unevenly distributed among seasons, roughly ranging from 400 to 800 mm, and more than 70% of precipitation events occur in the summer during the maize growing season. Both temperature and precipitation decrease gradually from southeast to northwest. As shown in Figure 1a, nearly half of the region is planted with crops, and the prevailing double-cropping system is winter wheat and summer maize. Due to insufficient precipitation in spring and winter, supplemental irrigation for winter wheat is required to obtain optimum yields. As a result, Henan suffers from serious water shortages and environmental problems related to groundwater overexploitation. Therefore, strengthening soil moisture monitoring in the agriculture areas is of great significance for improving water use efficiency in this province.

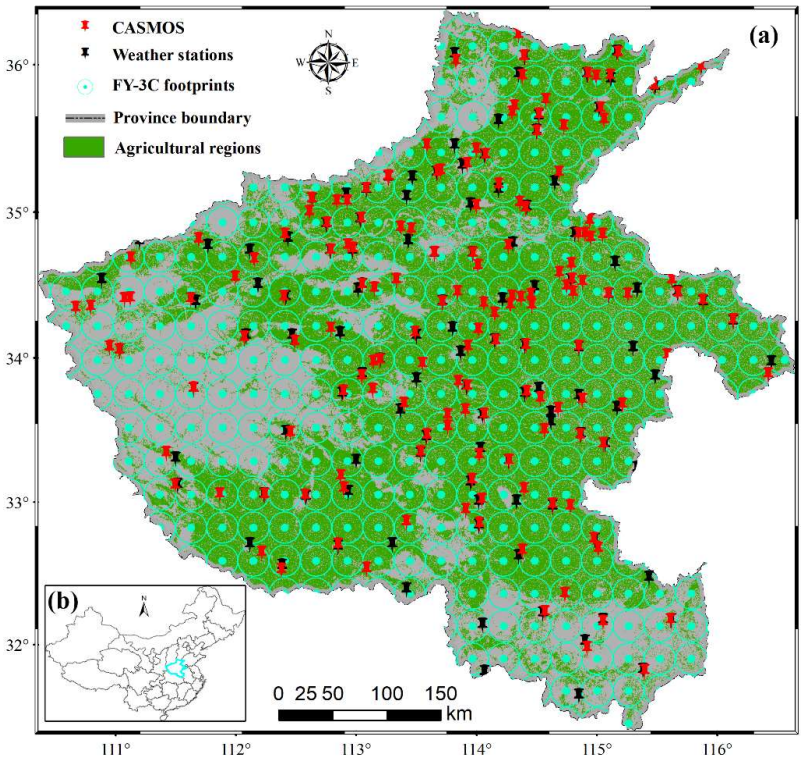

Figure 1. (a) The agricultural regions, Chinese Automatic Soil Moisture Observation Stations (CASMOS), the weather stations, and the footprints of Fengyun-3C (FY-3C) located in Henan province; (b) The location of Henan province in China.

2.2. FY-3C L2 Soil Moisture Product

The FY-3 satellite series is China's second-generation polar-orbiting satellites and includes four satellites, FY-3A, FY-3B, FY-3C, and FY-3D, with an approximately two-year separation between two subsequent launches [11]. The first two experimental satellites, FY-3A and FY-3B, were successfully

launched on May 27, 2008 and December 5, 2010, respectively, whereas FY-3C and FY-3D were respectively sent into orbit on September 23, 2013 and November 14, 2017 [22]. FY-3A and FY-3C orbit midmorning with their local solar time on descending node (LTDN) around 10:00 a.m., whereas FY-3B and FY-3D orbit in the afternoon with their local solar time on ascending node (LTAN) around 2:00 p.m. [27].

The band information for the MWRI aboard FY-3A, FY-3C, FY-3B, and FY-3D is listed in Table 1. The FY-3 L2 soil moisture products are described in volumetric water content in m^3/m^3, which are retrieved from the brightness temperatures collected by the MWRI using a similar algorithm as the AMSR-E soil moisture product [13]. Since the soil moisture product is not available for FY-3D, in this study, we used the soil moisture product from FY-3C for evaluation, which is thought to have the highest observation accuracy in the series.

Table 1. Introduction to the microwave radiation imager channels.

Frequency (GHz)	Polarization	Bandwidth (MHz)	Sensitivity (K)	IFOV km × km	Pixel Size km × km
10.65	V/H	180	0.5	51 × 85	40 × 11.2
18.70	V/H	200	0.5	30 × 50	40 × 11.2
23.80	V/H	400	0.8	27 × 45	20 × 11.2
36.50	V/H	900	0.5	18 × 30	20 × 11.2
89.00	V/H	4600	1.0	9 × 15	10 × 11.2

Note: V is vertical polarization; H is horizonal polarization; IFOV is the instantaneous field of view.

The FY-3C L2 soil moisture products are available from May 2014 to present (2018). They include three products with different time scales: daily, 10-day average, and monthly average, each of which separately includes two subsets: one from the ascending orbits (10:00 p.m. local time) and the other from descending orbits (10:00 a.m. local time). In this study, the daily product, combining both the ascending and descending datasets, was used. If the two datasets overlapped, their averaged value was used. All the L2 soil moisture products are posted on a 25-km Equal Area Scalable Earth-1 (EASE1) grid [28], and the footprints of the products in our study region are plotted in Figure 1a. According to the documents of the products, FY-3C L2 SM products provide the amount of soil moisture of the top 5-cm layer, with a desired estimation accuracy of 0.06 m^3/m^3 [13].

2.3. In Situ Soil Moisture Measurements

To improve the ability of drought monitoring and early disaster warning for the agricultural regions in China, since 2009, an extensive national soil moisture collecting network, CASMOS, has been developed by the Chinese Meteorological Administration (CMA) [29]. After several years of construction, more than 2000 observation stations have been set up in the agricultural areas of the country. Most of the observations contain eight measurement depths: 0–10, 10–20, 20–30, 30–40, 40–50, 50–60, 70–80, and 90–100 cm. The elements observed include soil volumetric water content, relative soil humidity, soil weight water content, and soil available water storage. Three types of observation instruments, DNZ1, DNZ2, and DNZ3, are separately produced by Shanghai Changwang Meteorological Science and Technology Corporation (Shanghai, China), Henan Meteorological Science Research Institute and the 27th Institute of China National Electric Power Corporation (Zhengzhou, China), and China Huayun Technology Development Corporation (Beijing, China) [30]. The operating principle of these three types of instruments is based on the frequency reflection method. DNZ1, which was set up in Henan, uses the standing wave method, whereas DNZ2 and DNZ3 use the capacitance method [31].

The in-situ soil moisture measurements we used in this paper were collected from the 158 monitoring stations in Henan province from January 1 to December 31, 2016. As displayed in Figure 1a, the observation stations covered more than 120 counties in the province and formed an effective soil moisture monitoring network for the agricultural areas [32]. The Meteorological Observation Centre of CMA is in charge of data archiving and distribution. The CMA records the measurements

every hour, and then the daily averaged values are produced from these data. For comparison with the depth of FY-3C soil moisture, we only used the soil moisture data from the 0–10-cm layer.

2.4. MODIS NDVI and Precipitation Data

Moderate Resolution Imaging Spectroradiometer (MODIS) Normalized Difference Vegetation Index (NDVI), produced on 16-day intervals and at several spatial resolutions, enables consistent spatial and temporal comparisons of vegetation canopy greenness, which is a composite property of leaf area, chlorophyll, and canopy structure [33]. In this study, we used the MODIS NDVI product consisting of MYD13Q1 from the Aqua satellite and MOD13Q1 from the Terra satellite, both of which were retrieved from daily, atmosphere-corrected, and bidirectional surface reflectance with a spatial resolution of 250 m [34,35]. As the MODIS sensors aboard these two satellites are identical, the NDVI algorithm generates each 16-day composite 8 days apart, which permits a higher temporal resolution product by combining both products. Figure 2 displays how the combined NDVI varied during a one-year period around the observation station of O2007, which is located within a typical agricultural region. MYD13Q1 started on January 9, 2016, and MOD13Q1 began on January 17, 2016. As shown in the figure, higher NDVI values corresponded with the crop growing periods with larger biomass; for winter wheat, these months were April and May, whereas for summer maize, these months were July, August, and September.

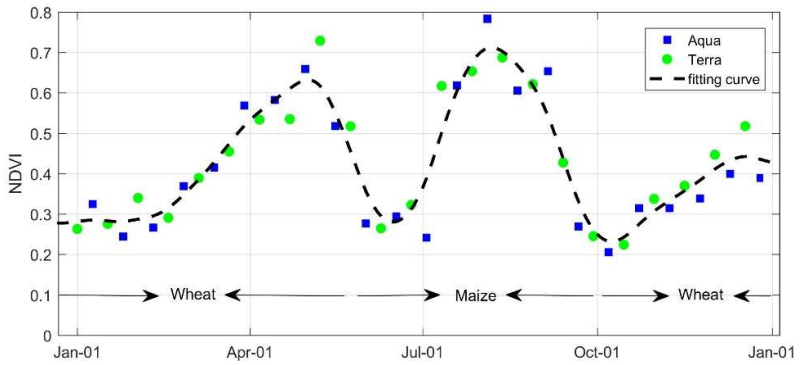

Figure 2. Normalized Difference Vegetation Index (NDVI) variations in 2016 at station O2007. The blue squares represent NDVI from Aqua, the green circles represent NDVI from Terra, and the black dashed line represents the fitting curve of the combined NDVI. The combined NDVI measurements were fitted using spline smoothing methods in the MATLAB Curve Fitting Toolbox, with a smoothing parameter of 0.001.

Precipitation events are the most important factors determining the surface soil, and precipitation data can assist in validating the soil products derived from satellites [36]. We extracted the precipitation data from the China National Surface Weather Station Normalized Precipitation Dataset Version 3.0, which is archived by the Chinese Meteorological Data Service Centre (CMDSC, http://data.cma.cn). As shown in Figure 1a, in Henan province, there are 119 national weather collecting stations. In the dataset, the rainfall data are provided in mm/hour, and daily averaged rainfall was further obtained based on the original data.

3. Methodology

As introduced above, many previous studies have evaluated different satellite-based soil moisture products using in situ soil moisture measurements [2,3,5,17,21]. In this paper, with the assistance of in situ soil moisture data from CASMOS and other auxiliary datasets, like rainfall and NDVI, we assessed the performance of the FY-3C L2 SM product in the agricultural regions of Henan province and analyzed factors that influence the results. We employed four statistics to verify the effectiveness of the FY-3C product: the mean difference (MD), the root-mean-square error (RMSE), the unbiased RMSE (ubRMSE), and the correlation coefficient (R).

3.1. Study Framework and Data Integration

Figure 3 summarizes the workflows of this analytical framework. As shown in the figure, aside from the soil moisture data from the FY-3C MWRI, the three datasets introduced in Section 2—soil moisture measurements from CASMOS, rainfall from weather stations, and NDVI from MODIS—were integrated into the framework as well. However, these four datasets were different in both their spatial and temporal scales. For example, the soil moisture data from CASMOS and rainfall data were point measurements and daily averaged data were available nearly every day during the evaluation period. For MODIS NDVI and the FY-3C MWRI soil product, their spatial resolutions were 250 m and 25 km, respectively, and their temporal intervals were 2–3 and 8 days, respectively. Thus, the manner in which these datasets were integrated was crucial for the FY-3C soil moisture evaluation and later analysis.

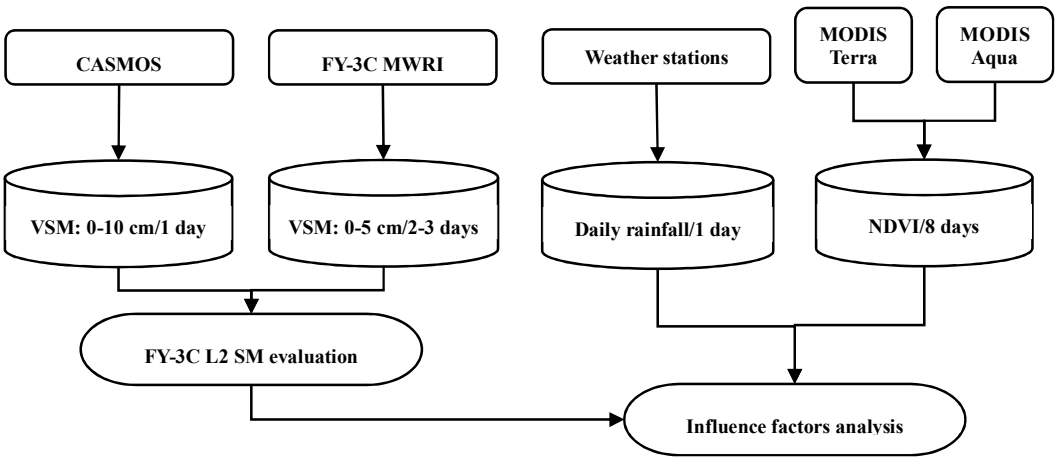

Figure 3. Work flowchart of this study. CASMOS represents the Chinese Automatic Soil Moisture Observation Stations deployed in the study area; MWRI represents the microwave radiation imager aboard the FY-3C satellite; VSM indicates the volumetric soil moisture with the unit in m^3/m^3.

When integrating the datasets, only those footprints that contained monitoring stations were used for evaluation. We generally extracted other datasets on the spatial scale based on the footprints of the FY-3C L2 soil moisture product (Figure 1a). In situ data, including the soil moisture and the rainfall measurements, which lay within an FY-3C soil moisture footprint, were considered the corresponding ground truth for the region. If there was more than one station within a footprint, the averaged values were used. When extracting the NDVI data to match the resolution of the FY-3C soil moisture product, all the NDVI values within a footprint were averaged. Notably, some of the CASMOS were located in cities. These stations cannot correctly reflect the soil moisture information of the surrounding agricultural areas, and the satellite inversion results are heavily affected by the buildings. Therefore, the 42 observation stations located in cities were excluded. Temporally, only the dates when half of our study region had FY-3C soil moisture observation data were used in our evaluation and analysis. To temporally agree with the FY-3C data, in situ soil moisture and rainfall data of these dates were extracted, and the NDVI data were interpolated to the dates.

3.2. Four Statistical Indicators

The MD represents the bias, which is the systematic difference between satellite soil moisture retrievals and in situ soil moisture measurements. The MD can be obtained using the following equation:

$$\mathrm{MD} = \frac{\sum_{i=1}^{N}\left(\mathrm{mv}_i^{\mathrm{fy}} - \mathrm{mv}_i^{\mathrm{sta}}\right)}{N} \quad (1)$$

The RMSE represents the absolute difference or accuracy of FY-3C soil moisture retrievals relative to in situ soil moisture measurements, which can be calculated as:

$$\mathrm{RMSE} = \sqrt{\frac{\sum_{i=1}^{N}\left(\mathrm{mv}_i^{\mathrm{fy}} - \mathrm{mv}_i^{\mathrm{sta}}\right)^2}{N}} \quad (2)$$

where $\mathrm{mv}_i^{\mathrm{fy}}$ represents FY-3C soil moisture retrieval (m^3/m^3), $\mathrm{mv}_i^{\mathrm{sta}}$ is the in situ soil moisture measurement (m^3/m^3), N represents the total number of samples, and i represents a specific sample. For temporal analysis, N varied for each grid cell and only dates that had valid data from both datasets were used for calculation. For spatial analysis, N varied for each date and only stations that had valid data from both datasets were used for calculation.

To better evaluate the estimation of the absolute difference of FY-3C soil moisture, we adopted the ubRMSE, which removes the bias of RMSE that characterizes random error. The ubRMSE is calculated using the following equation [37]:

$$\mathrm{ubRMSE} = \sqrt{\mathrm{RMSE}^2 - \mathrm{MD}^2} \quad (3)$$

The correlation coefficient R indicates the relative accuracy between FY-3C soil moisture data and in situ soil moisture measurements. The R between the FY-3C soil moisture data and in situ soil moisture can be expressed as the following formula:

$$R = \frac{\sum_{i=1}^{N}(\mathrm{mv}_i^{\mathrm{fy}} - \overline{\mathrm{mv}}^{\mathrm{fy}})(\mathrm{mv}_i^{\mathrm{sta}} - \overline{\mathrm{mv}}^{\mathrm{sta}})}{(N-1)\sigma^{\mathrm{fy}}\sigma^{\mathrm{sta}}} \quad (4)$$

where $\overline{\mathrm{mv}}^{\mathrm{fy}}$ is the FY-3C soil moisture average (m^3/m^3) during the whole evaluation period within one grid for temporal analysis, or of the valid stations in 1 day for spatial analysis; $\overline{\mathrm{mv}}^{\mathrm{sta}}$ indicates the average of in situ soil moisture measurements (m^3/m^3); σ^{fy} and σ^{sta} are the standard deviation of satellite and in situ soil moisture (m^3/m^3), respectively.

4. Results

In this section, the statistical accuracy indicators of FY-3C L2 SM retrievals are presented in both temporal and spatial scales. During the comparison, the in situ SM measurements from CASMOS were treated as the ground truth for FY-3C L2 SM. The nighttime (ascending) microwave satellite data were generally expected to produce more accurate soil moisture estimates than the daytime (descending) data. However, many previous studies proved that there were no significant differences between the soil moisture from daytime and nighttime overpasses [2,38]. Thus, we simply ignored the diurnal differences in this study. In Section 4.1, we examine the temporal performance of the FY-3C L2 product during the one-year period for each footprint in our study region; in Section 4.2, we evaluate the spatial performance of the footprints available for each date during the year.

4.1. Temporal Performance for Different Footprints

To understand the temporal agreement and consistency between FY-3C satellite retrievals and in situ measurements of different footprints, the four accuracy indicators for each valid footprint in our study area were first computed separately. For example, we took the footprint that covered station O2342. As shown in Figure 4, the daily average soil moisture from FY-3C and the monitoring station were plotted in time over the entire assessment period. The four statistical indicators were calculated using the dates when the two data sets were both available. For this footprint, the MD, RMSE, and ubRMSE were -0.02, 0.11, and 0.11 m^3/m^3, respectively, and the correlation coefficient R

was 0.21. Note that the MD indicator was calculated by subtracting the in situ SM measurement value from the FY-3C SM value. A positive bias value indicates that the FY-3C soil moisture retrieval is larger (wetter) than the in situ observation, whereas a negative value indicates that the FY-3C SM retrieval is lower (drier) than the in situ observation.

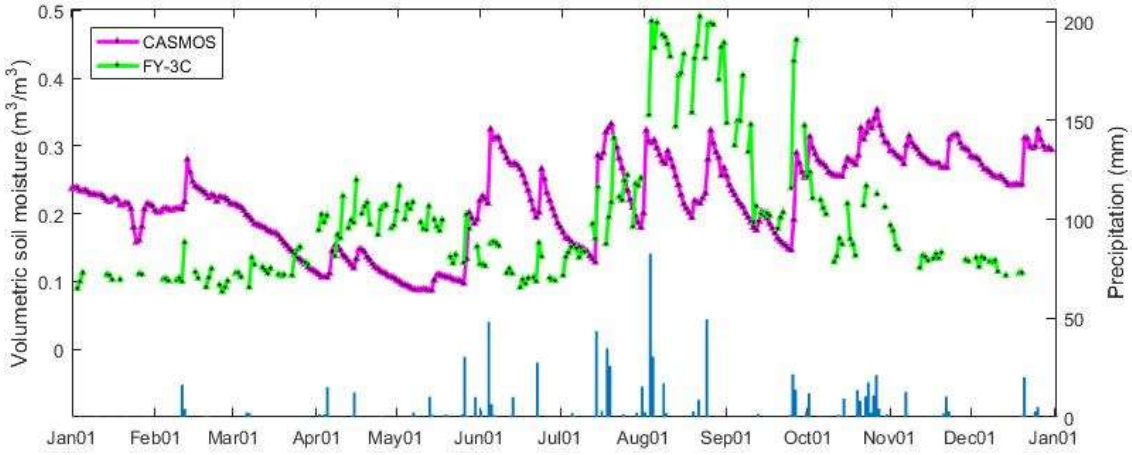

Figure 4. Temporal variations in the soil moisture data from the CASMOS and the FY-3C, and the rainfall data around the O2342 station during 2016. The orange line is the soil moisture (SM) daily mean from the CASMOS, the green line represents the SM daily mean of the FY-3C L2 product, and the blue histogram represents the daily precipitation.

Using the abovementioned method, we then separately calculated the statistical indicators between the two SM datasets for all the footprints. Figure 5 gives the histograms of the four statistical indicators for all the stations regardless of their location. Overall, the FY-3C soil moisture retrievals were lower than the in situ measurements, with an average bias of −0.050 m^3/m^3. From the figure, FY-3C SM generally showed a bias of about −0.05 m^3/m^3; FY-3C SM had a large derivation from the in situ station SM, with an average RMSE of 0.11 m^3/m^3 and a ubRMSE of 0.085 m^3/m^3. They were weakly correlated, with an average value of 0.092.

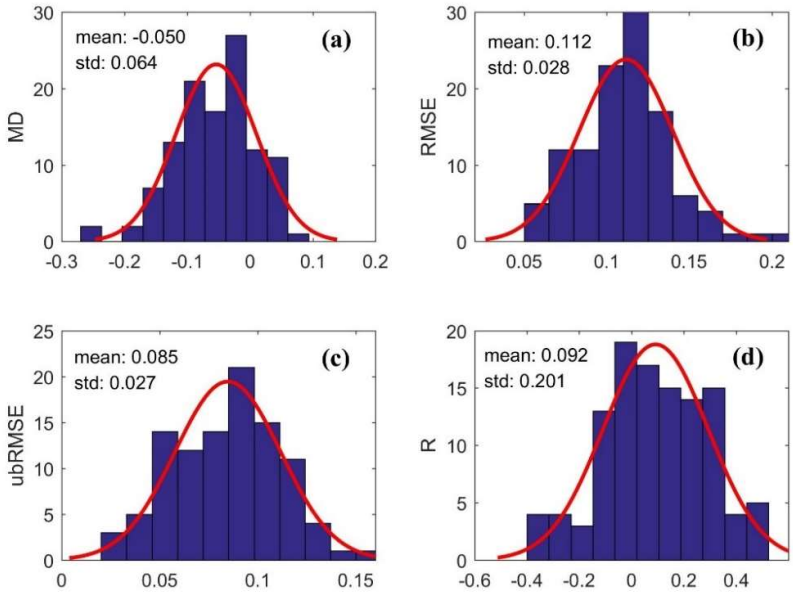

Figure 5. The temporal statistical indices between the two soil moisture datasets from the FY-3C MWRI and the in situ stations: (a) Mean difference (MD), (b) root-mean-square error (RMSE), (c) unbiased RMSE (ubRMSE), and (d) correlation coefficient(*R*).

Figure 5 also shows that the temporal consistency between the two datasets was different for different footprints. To further illustrate how their consistency varied spatially, the statistical indicators were interpolated to the extent of our study area with a spatial resolution of 0.25° (Figure 6). The interpolations were carried out in ArcGIS software (Esri, NewYork, USA) using the Kriging method. In general, for most grid cells, their biases were negative (see green and yellow colours in Figure 6a), approximately ranging from –0.1 to –0.03 m^3/m^3. In terms of RMSE and ubRMSE, they shared a similar distribution pattern, in which most grid cell high values were located in the eastern part of Henan (Figures 6b,6c), suggesting that the FY-3C SM retrievals were more consistent with in situ measurements in the western part than in the eastern agricultural regions in Henan (Figure 1). Similarly, the grid cells with higher correlation coefficients (red color in Figure 6d) were located in Western Henan. However, there were some exceptional regions. For example, in the southeast part of Henan a positive bias, larger RMSE and ubRMSE, as well as higher correlation were recorded.

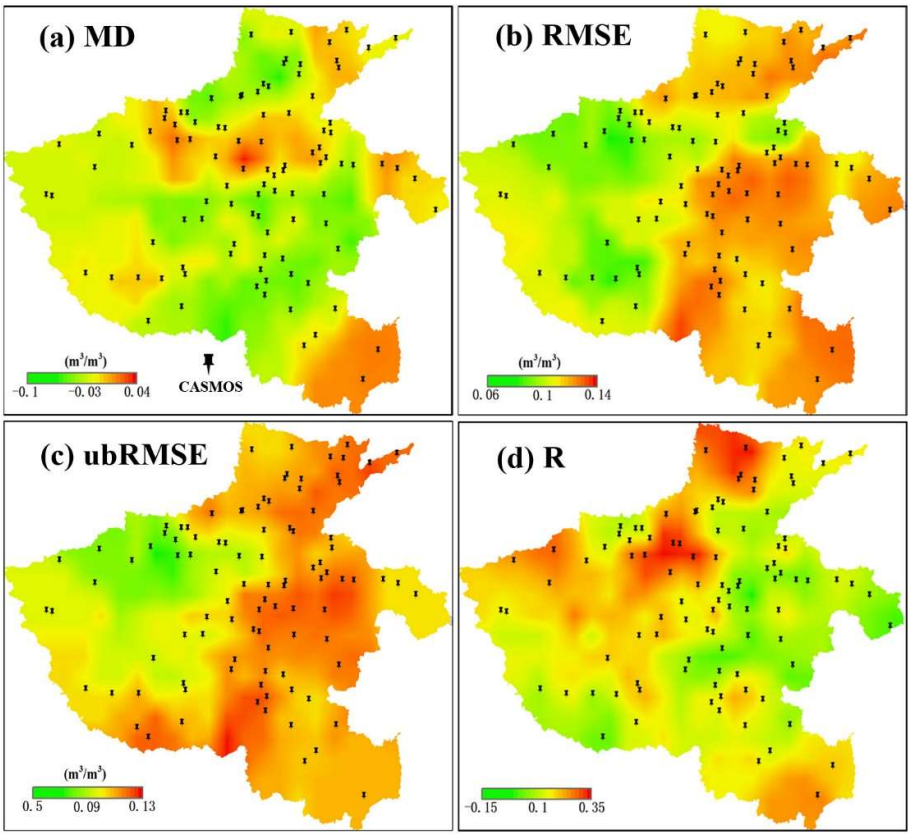

Figure 6. The spatial distribution difference between the FY-3C retrievals and in situ measurements for the period of January 1 to December 31, 2016: (a) MD, (b) RMSE, (c) ubRMSE, and (d) *R*. The black thumbtacks represent the locations of the in situ soil moisture stations (CASMOS).

4.2. Spatial Performance At Different Times

We continued to evaluate the spatial performance of the FY-3C SM product at different times of the year. As shown in Figure 7, four dates (March 8, June 2, August 9, and October 2, 2016) were picked to display the typical performance of FY-3C SM against in situ SM measurements (CASMOS) in different seasons. The four statistical indicators between the two datasets on different dates (Figure 7) indicated that the temporal variation was a key factor influencing FY-3C SM performance. For example, on 8 March, 2 June, and 2 October 2016, the FY-3C SM, in contrast with the in situ data, underestimated the soil moisture by different degrees, whereas it highly overestimated the soil moisture on 9 August 2016.

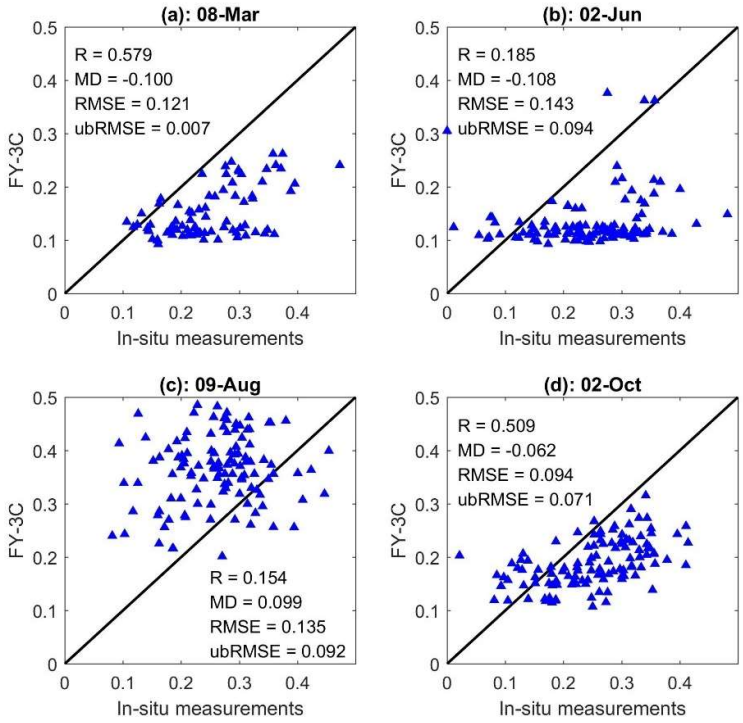

Figure 7. The FY-3C SM product versus in situ SM measurements (CASMOS) on four different dates in 2016.

We evaluated the FY-3C SM L2 product performance against in situ SM measurements of all the valid dates (if more than half of the CASMOS stations had corresponding FY-3C SM observing data within a date, we defined the date as a valid date) during the year. Figure 8 displays the distributions of the four indicators for all available dates, from which we can see that the consistency between the two datasets was generally poor. The average values of MD, RMSE, ubRMSE, and *R* were –0.043 m^3/m^3, 0.112 m^3/m^3, 0.073 m^3/m^3, and 0.214, respectively. However, compared with the temporal performance of the different footprints (Figure 5), the FY-3C SM L2 product showed better consistency with the CASMOS measurements on the spatial scale (Figure 8). For example, the average MD dropped from –0.050 to –0.043 m^3/m^3, and the average correlation coefficient *R* rose to 0.214 from 0.092.

Preprints (www.preprints.org) | NOT PEER-REVIEWED | Posted: 5 December 2018 doi:10.20944/preprints201812.0068.v1

Peer-reviewed version available at Water 2019, 11, 248; doi:10.3390/w11020248

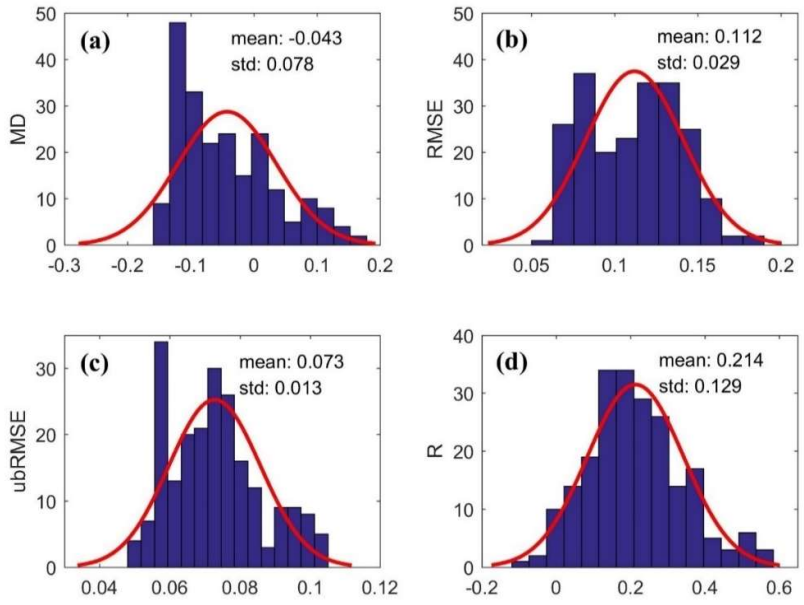

Figure 8. The spatial statistical indices between the two soil moisture datasets from the FY-3C MWRI and the in situ stations: (a) MD, (b) RMSE, (c) ubRMSE, and (d) *R*.

Next, a more specific analysis was conducted to examine the temporal evolution of the statistical parameters between the compared datasets (Figure 9 and Table 2). As shown in the figure, the varying patterns of the four indicators over time during the year were generally different. The MD showed a double-peak trend, with peaks around May and August (Figure 9a). Except for the peaks, basically on all dates, FY-3C SM retrievals showed a negative bias compared to the in situ observations, further indicated by the monthly mean bias data in Table 2. The monthly mean bias across the year ranged from −0.11 to 0.08 m^3/m^3, with an average value of −0.04 m^3/m^3. This underestimation has also been revealed by many previous validation studies [3,23,39] for the soil moisture products of AMSR-E and AMSR2, which were derived using a similar retrieving algorithm as that used for the FY-3C L2 product.

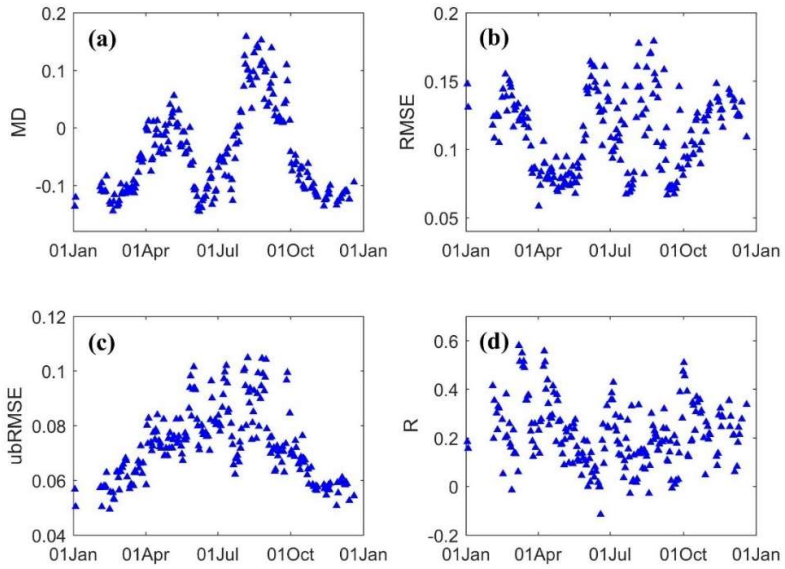

Figure 9. Temporal evolution of the statistical parameters between SM of in situ monitoring stations and FY-3C in 2016. As introduced in Figure 5, the MD was calculated by subtracting the in situ SM from FY-3C.

Table 2. Monthly averaged statistics for FY-3C daily average soil moisture retrievals against in situ observations. Mean difference (MD), root-mean-square error (RMSE), and unbiased RMSE (ubRMSE) are in m^3/m^3.

	Jan	Feb	Mar	Apr	May	Jun	Jul	Aug	Sep	Oct	Nov	Dec	Mean
MD	-0.11	-0.10	-0.09	-0.04	0.02	-0.05	-0.05	0.08	0.05	-0.08	-0.10	-0.11	-0.04
RMSE	0.13	0.13	0.11	0.08	0.08	0.12	0.12	0.13	0.10	0.11	0.12	0.13	0.11
ubRMSE	0.06	0.06	0.06	0.07	0.08	0.09	0.09	0.09	0.08	0.06	0.06	0.06	0.07
R	0.19	0.21	0.22	0.27	0.12	0.05	0.12	0.09	0.08	0.21	0.24	0.25	0.21

Regarding the RMSE, the values roughly ranged from 0.08 to 0.13 m^3/m^3, with an average of 0.11 m^3/m^3 (Table 2), indicating inconsistency between the two datasets. Seasons were one factor influencing the RMSE (Figure 9b), but the variation behaviors were different from the MD and thus not easy to understand. For most of the year, the RMSE tended to be higher than 0.1 m^3/m^3, except for April, May, and some dates in the autumn. The daily and monthly average ubRMSE (Figure 9c and Table 2) show that spring (January–March) and winter (October–December) had the smallest average values (0.06 m^3/m^3), and the dates from May to August had the largest average ubRMSE (0.08–0.09 m^3/m^3), which may imply that ground vegetation density is a key factor determining the FY-3C SM performance. Low correlations (R < 0.2) between FY-3C retrievals and in situ measurements were found for most times of the year, indicating poor temporal consistency between the two compared datasets in our study area. The positive correlation coefficient (0.21) computed in our study was a bit lower than the reported results in previous satellite-derived SM products evaluation studies. For example, an R value of 0.24 was computed in Wu et al. [3], 0.31 in Cho et al. [40], and 0.38 in Kim et al. [41].

5. Discussion

In this study, we investigated the estimated error of the FY-3C remotely sensed SM product against in situ soil moisture measurements from the CASMOS on both temporal and spatial scales. As conventionally performed in previous studies [2-4,16] , during our analysis, the in situ soil moisture measurements were used as ground truth to evaluate FY-3C L2 soil moisture retrievals. With point-scale data, there may be several limitations during comparisons with larger footprint-scale satellite data. The monitoring stations supply soil moisture measurements at point locations, whereas the FY-3C MWRI sensor measures the average soil moisture within one satellite footprint. Due to the coarse resolution (25 km) of the FY-3C SM product and the spatial heterogeneity of the surface soil moisture, we cannot use point-based in situ measurements to correctly represent the spatially averaged soil moisture within a 25-km satellite footprint [42]. . The in situ soil moisture measurements used in our evaluation were sourced from the station sensors deployed at a depth of 10 cm below the soil surface. FY-3C MWRI can only sense the soil moisture signal from the top soil layer (approximately 1–2 cm), which implies that FY-3C retrievals may not dependably represent the soil moisture in much deeper layers than the sensing depth. Additionly, other factors such as vegetation coverage, precipitation, and climate characteristics also influence the evaluation results, and their temporal and dynamic variation would lead to different levels of performance in the spatiotemporal analysis [2]. Considering the above, we could not expect FY-3C retrievals to exactly match the in situ measurements from the CASMOS monitoring stations even under ideal conditions [3].

After investigating the evaluated results in Section 4, FY-3C SM retrievals generally exhibited poor consistency with the in situ soil moisture measurements. The average MD between the FY-3C soil moisture estimates and the in situ soil moisture measurements ranged from −0.11 to 0.08 m^3/m^3. Other statistical indicators—RMSE, ubRMSE, and R—also validated the large differences between the products. For some regions in Henan (Figure 6) and during some months of the year (Figure 9), they even displayed large estimated errors and negative correlations at the same time. Similarly, poor performance was observed when validating the AMSRE and AMSR2 soil moisture products [2,41], which were derived using a retrieving algorithm similar to the FY-3C SM product. The limited

parameterizations and uncertainties of the radiative transfer model used in the soil moisture retrieval and the inconsistency in sensing depth between the remotely sensed data and the in situ measurements are generally thought to contribute to the inconsistency [43] and are applicable to FY-3C L2 SM product.

The official SM retrieval algorithm in FY-3C may also contribute to the poor results. The algorithm [9,44], which was set up based on the tau-omega model [43], makes a further simplification where the polarization-reducing effect of vegetation is assumed to be constant over a long period [45], which effectively keeps the vegetation water content constant. Simultaneously, the algorithm makes use of two frequencies, 10.65 and 18 GHz, to describe the parameterization of the vegetation. The algorithm, as a result, ascribes all deviations in the microwave polarization difference index (MPDI) from vegetation variations in the scene to a change in soil moisture [13]. That is, the soil moisture retrieved from the FY-3C MWRI is closely related to the amount of vegetation in one footprint.

The increase in uncertainty in FY-3C soil moisture products with increasing vegetation was theoretically expected and was widely confirmed in our analysis of the soil moisture products. For instance, the temporal performance of the FY-3C SM product for the footprints in Western Henan showed better agreement than the footprints in Eastern Henan, which is dominated by agricultural regions. The spatial performance at different times of the year was closely related to the seasons (e.g., the daily mean bias between the two datasets showed a double-peak variation pattern, tended to overestimate the soil moisture in May, August, and September, and underestimated the soil moisture during the rest of the year.) This varying trend aligns with the cropping system in Henan, where winter wheat and summer maize reach their vegetation density maximum in May and August, respectively. Here, we used the NDVI collected from the MODIS satellites (Section 2.4.) to represent the ground vegetation density. Figure 10 depicts the temporal variations in the FY-3C SM and MODIS NDVI for the FY-3C footprint covering the CASMOS station O2073, demonstrating that the two datasets shared a similar temporal varying trend and that the influence of vegetation could be captured by using a time-series-based approach to soil moisture assessment [46].

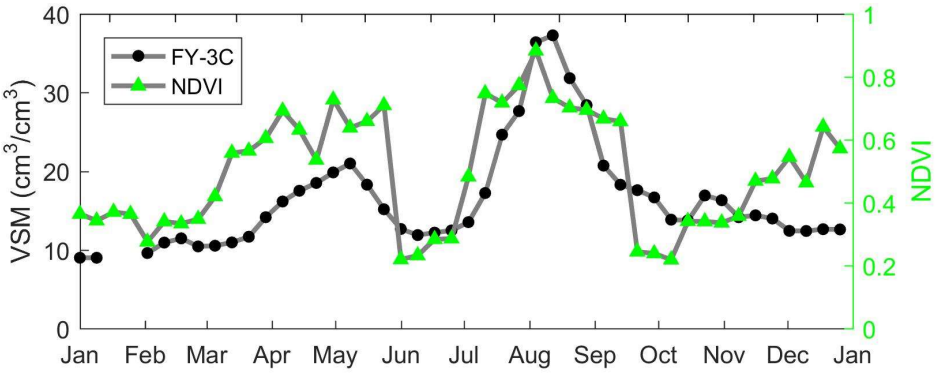

Figure 10. The temporal variations in FY-3C soil moisture and MODIS NDVI around the O2073 station in 2016. The green triangles represent the average NDVI of the footprint which covers the O2073 station; the black circles represent the FY-3C soil moisture retrievals of the footprint.

We calculated the temporal correlation coefficients (R) between the FY-3C L2 SM and MODIS NDVI for all the footprints in Henan. As shown in Figure 11, FY-3C SM was closely related to MODIS NDVI, with an average R of 0.55, which is consistent with the findings of several previous studies [2,13,47]. As in Henan province, especially in the agricultural regions, the cropping system dominates the NDVI variations throughout the year. The strong correlation between the two products revealed that the cropping system had a considerable influence on the soil moisture retrievals, which simultaneously quantitatively explained the influence of the crops on the soil moisture products. To improve the accuracy of the FY-3C soil moisture product, an improved algorithm that could filter out the influences of the crops should be developed in future studies.

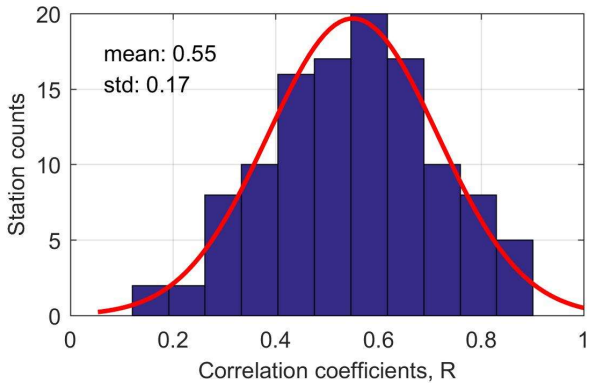

Figure 11. Histogram of the correlation coefficients between FY-3C SM and NDVI for all stations.

6. Conclusions

We preliminary evaluated the FY-3C level 2 daily soil moisture product in Henan province in China using in situ data from 158 soil moisture monitoring stations deployed by the CMA Meteorological Observation Centre. Our analysis revealed that the FY-3C L2 soil moisture retrievals had a bias around –0.04 m^3/m^3 compared to in situ measurements at depths of 0–10 cm. If the in situ measurements were treated as ground truths, the absolute accuracy of FY-3C soil moisture retrievals was 0.11 m^3/m^3 (RMSE), which is much worse than the desired accuracy of 0.06 m^3/m^3.

The FY-3C L2 SM product tends to overestimate the soil moisture amount when the crop biomass is large in May, August, and September and underestimates soil moisture during the rest of the year. This result agrees with our expectation because vegetation water considerably influences passive microwave soil moisture retrievals in the footprint. In conclusion, the accuracy and reliability of the FY-3C soil moisture estimates in agricultural areas depend upon the crop types as well as their growing stages. This issue should be addressed in future studies to improve the accuracy of FY-3C soil moisture estimates.

Author Contributions: Conceptualization, Yongchao Zhu and Shibo Fang; Formal analysis, Yongchao Zhu, Dongli Wu and Ruijing Sun; Funding acquisition, Simon Pearson and Shibo Fang; Methodology, Yongchao Zhu, Dongli Wu and Ruijing Sun; Project administration, Simon Pearson and Shibo Fang; Resources, Simon Pearson and Shibo Fang; Writing – original draft, Yongchao Zhu; Writing – review & editing, Simon Pearson, Dongli Wu, Ruijing Sun and Shibo Fang.

Funding: This research was funded by the Project of International Cooperation and Exchanges NSFC (NSFC-RCUK_STFC) (61661136005) and the NSFC Program (41490633) the UK STFC Program (ST/N006836/1).

Acknowledgments: The authors wish to thank NSMC, CMDSC and NSDIC for making the soil moisture and the precipitation and the NDVI data available online.

Conflicts of Interest: The authors declare no conflict of interest.

Reference

1. Makkeasorn, A.; Chang, N.B.; Beaman, M.; Wyatt, C.; Slater, C. Soil moisture estimation in a semiarid watershed using radarsat - 1 satellite imagery and genetic programming. *Water Resources Research* **2006**, *42*, W09401.
2. Zhang, X.; Zhang, T.; Zhou, P.; Shao, Y.; Gao, S. Validation analysis of smap and amsr2 soil moisture products over the united states using ground-based measurements. *Remote Sensing* **2017**, *9*, 104.
3. Wu, Q.; Liu, H.; Wang, L.; Deng, C. Evaluation of amsr2 soil moisture products over the contiguous united states using in situ data from the international soil moisture network. *International Journal of Applied Earth Observation and Geoinformation* **2016**, *45*, 187-199.
4. Karthikeyan, L.; Pan, M.; Wanders, N.; Kumar, D.N.; Wood, E.F. Four decades of microwave satellite soil moisture observations: Part 1. A review of retrieval algorithms. *Advances in Water Resources* **2017**, *109*, 106-120.
5. Kang, C.S.; Kanniah, K.D.; Kerr, Y.H.; Cracknell, A.P. Analysis of in-situ soil moisture data and validation of smos soil moisture products at selected agricultural sites over a tropical region. *International Journal of Remote Sensing* **2016**, *37*, 3636-3654.
6. Kerr, Y.H.; Waldteufel, P.; Richaume, P.; Wigneron, J.P.; Ferrazzoli, P.; Mahmoodi, A.; Al Bitar, A.; Cabot, F.; Gruhier, C.; Juglea, S.E. The smos soil moisture retrieval algorithm. *IEEE Transactions on Geoscience and Remote Sensing* **2012**, *50*, 1384-1403.
7. Entekhabi, D.; Njoku, E.G.; O'Neill, P.E.; Kellogg, K.H.; Crow, W.T.; Edelstein, W.N.; Entin, J.K.; Goodman, S.D.; Jackson, T.J.; Johnson, J. The soil moisture active passive (smap) mission. *Proceedings of the IEEE* **2010**, *98*, 704-716.
8. Kawanishi, T.; Sezai, T.; Ito, Y.; Imaoka, K.; Takeshima, T.; Ishido, Y.; Shibata, A.; Miura, M.; Inahata, H.; Spencer, R.W. The advanced microwave scanning radiometer for the earth observing system (amsr-e), nasda's contribution to the eos for global energy and water cycle studies. *IEEE Transactions on Geoscience and Remote Sensing* **2003**, *41*, 184-194.
9. Njoku, E.G.; Jackson, T.J.; Lakshmi, V.; Chan, T.K.; Nghiem, S.V. Soil moisture retrieval from amsr-e. *IEEE transactions on Geoscience and remote sensing* **2003**, *41*, 215-229.
10. Imaoka, K.; Kachi, M.; Kasahara, M.; Ito, N.; Nakagawa, K.; Oki, T. Instrument performance and calibration of amsr-e and amsr2. *International Archives of the Photogrammetry, Remote Sensing and Spatial Information Science* **2010**, *38*, 13-18.
11. Zhang, P.; Yang, J.; Dong, C.; Lu, N.; Yang, Z.; Shi, J. General introduction on payloads, ground segment and data application of fengyun 3a. *Frontiers of Earth Science in China* **2009**, *3*, 367-373.
12. Yang, J.; Zhang, P.; Lu, N.; Yang, Z.; Shi, J.; Dong, C. Improvements on global meteorological observations from the current fengyun 3 satellites and beyond. *International Journal of Digital Earth* **2012**, *5*, 251-265.
13. Parinussa, R.; Wang, G.; Holmes, T.; Liu, Y.; Dolman, A.; De Jeu, R.; Jiang, T.; Zhang, P.; Shi, J. Global surface soil moisture from the microwave radiation imager onboard the fengyun-3b satellite. *International journal of remote sensing* **2014**, *35*, 7007-7029.
14. Dorigo, W.A.; Scipal, K.; Parinussa, R.M.; Liu, Y.Y.; Wagner, W.; de Jeu, R.A.M.; Naeimi, V. Error characterisation of global active and passive microwave soil moisture data sets. *Hydrology and Earth System Sciences Discussions* **2010**, *7*, 5621-5645.

15. Wanders, N.; Karssenberg, D.; Bierkens, M.; Parinussa, R.; de Jeu, R.; van Dam, J.; de Jong, S. Observation uncertainty of satellite soil moisture products determined with physically-based modeling. *Remote Sensing of Environment* **2012**, *127*, 341-356.
16. Wang, S.; Mo, X.; Liu, S.; Lin, Z.; Hu, S. Validation and trend analysis of ecv soil moisture data on cropland in north china plain during 1981–2010. *International Journal of Applied Earth Observation and Geoinformation* **2016**, *48*, 110-121.
17. Petropoulos, G.P.; Ireland, G.; Srivastava, P.K.; Ioannou-Katidis, P. An appraisal of the accuracy of operational soil moisture estimates from smos miras using validated in situ observations acquired in a mediterranean environment. *International Journal of Remote Sensing* **2014**, *35*, 5239-5250.
18. Brocca, L.; Hasenauer, S.; Lacava, T.; Melone, F.; Moramarco, T.; Wagner, W.; Dorigo, W.; Matgen, P.; Martínez-Fernández, J.; Llorens, P. Soil moisture estimation through ascat and amsr-e sensors: An intercomparison and validation study across europe. *Remote Sensing of Environment* **2011**, *115*, 3390-3408.
19. Mladenova, I.; Lakshmi, V.; Jackson, T.J.; Walker, J.P.; Merlin, O.; de Jeu, R.A. Validation of amsr-e soil moisture using l-band airborne radiometer data from national airborne field experiment 2006. *Remote Sensing of Environment* **2011**, *115*, 2096-2103.
20. Jackson, T.J.; Bindlish, R.; Cosh, M.H.; Zhao, T.; Starks, P.J.; Bosch, D.D.; Seyfried, M.; Moran, M.S.; Goodrich, D.C.; Kerr, Y.H. Validation of soil moisture and ocean salinity (smos) soil moisture over watershed networks in the us. *IEEE Transactions on Geoscience and Remote Sensing* **2012**, *50*, 1530-1543.
21. Al-Yaari, A.; Wigneron, J.-P.; Ducharne, A.; Kerr, Y.; De Rosnay, P.; De Jeu, R.; Govind, A.; Al Bitar, A.; Albergel, C.; Munoz-Sabater, J. Global-scale evaluation of two satellite-based passive microwave soil moisture datasets (smos and amsr-e) with respect to land data assimilation system estimates. *Remote Sensing of Environment* **2014**, *149*, 181-195.
22. Tang, F.; Zou, X.; Yang, H.; Weng, F. Estimation and correction of geolocation errors in fengyun-3c microwave radiation imager data. *IEEE Transactions on Geoscience and Remote Sensing* **2016**, *54*, 407-420.
23. Jackson, T.J.; Cosh, M.H.; Bindlish, R.; Starks, P.J.; Bosch, D.D.; Seyfried, M.; Goodrich, D.C.; Moran, M.S.; Du, J. Validation of advanced microwave scanning radiometer soil moisture products. *IEEE Transactions on Geoscience and Remote Sensing* **2010**, *48*, 4256-4272.
24. Wagner, W.; Naeimi, V.; Scipal, K.; de Jeu, R.; Martínez-Fernández, J. Soil moisture from operational meteorological satellites. *Hydrogeology Journal* **2007**, *15*, 121-131.
25. De Jeu, R.; Wagner, W.; Holmes, T.; Dolman, A.; Van De Giesen, N.; Friesen, J. Global soil moisture patterns observed by space borne microwave radiometers and scatterometers. *Surveys in Geophysics* **2008**, *29*, 399-420.
26. Mason, P.; Reading, B. In *Implementation plan for the global observing systems for climate in support of the unfccc*, Proceedings of the 21st international conference on interactive information processing systems for meteorology, oceanography, and hydrology, 2005.
27. Han, Y.; Zou, X.; Weng, F. Cloud and precipitation features of super typhoon neoguri revealed from dual oxygen absorption band sounding instruments on board fengyun - 3c satellite. *Geophysical Research Letters* **2015**, *42*, 916-924.

28. Armstrong, R.; Brodzik, M. An earth-gridded ssm/i data set for cryospheric studies and global change monitoring. *Advances in Space Research* **1995**, *16*, 155-163.
29. Wu, D.; Cao, T.; Xue, H. The study of quality control for observing data of automatic soil moisture. *Journal of Soil Science* **2016**, *4*, 1-10.
30. Wu, D.; Liang, H.; Cao, T. China's automatic soil moisture observation network operation monitoring system construction. *Meterological Science and Technology (Chinese)* **2014**, *42*, 278-282.
31. Chen, H.; Ye, l.; Xue, L. Maintenance method of gstar-i (dzn2) type automatic soil moisture monitor and analysis of common faults. *Meterological and Environmental Sciences (Chinese)* **2011**, *34*, 178-181.
32. Xue, L.; Chen, H.; Shi, L. Construction and operation management of automatic soil moisture observation network in henan province. *Meteorological and Enveronmental Sciences* **2011**, *34*, 84-87.
33. Huete, A.; Didan, K.; van Leeuwen, W.; Miura, T.; Glenn, E. Modis vegetation indices. In *Land remote sensing and global environmental change*, Ramachandran B., J.C., Abrams M., Ed. Springer: New York, NY,USA, 2010; pp 579-602.
34. Lunetta, R.S.; Knight, J.F.; Ediriwickrema, J.; Lyon, J.G.; Worthy, L.D. Land-cover change detection using multi-temporal modis ndvi data. *Remote sensing of environment* **2006**, *105*, 142-154.
35. Huete, A.; Didan, K.; Miura, T.; Rodriguez, E.P.; Gao, X.; Ferreira, L.G. Overview of the radiometric and biophysical performance of the modis vegetation indices. *Remote sensing of environment* **2002**, *83*, 195-213.
36. Wagner, W.S., K.; Pathe, C.; Gerten, D.; Lucht, W.; Rudolf, B. Evaluation of the agreement between the first global remotely sensed soil moisture data with model and precipitation data. *Journal of Geophysical Research: Atmospheres* **2003**, *108*, 4611.
37. Entekhabi, D.; Yueh, S.; O'Neill, P.E.; Kellogg, K.H.; Allen, A.; Bindlish, R.; Brown, M.; Chan, S.; Colliander, A.; Crow, W.T. Smap handbook–soil moisture active passive: Mapping soil moisture and freeze/thaw from space. **2014**.
38. Kaihotsu, I.; Fujii, H.; Koike, T. In *Preliminary evaluation of amsr2 l3 soil moisture products using in situ observation data in mongolia*, AGU Fall Meeting Abstracts, 9-13 Decembe 2013.
39. Choi, M.; Hur, Y. A microwave-optical/infrared disaggregation for improving spatial representation of soil moisture using amsr-e and modis products. *Remote Sensing of Environment* **2012**, *124*, 259-269.
40. Cho, E.; Moon, H.; Choi, M. First assessment of the advanced microwave scanning radiometer 2 (amsr2) soil moisture contents in northeast asia. *Journal of the Meteorological Society of Japan. Ser. II* **2015**, *93*, 117-129.
41. Kim, S.; Liu, Y.Y.; Johnson, F.M.; Parinussa, R.M.; Sharma, A. A global comparison of alternate amsr2 soil moisture products: Why do they differ? *Remote Sensing of Environment* **2015**, *161*, 43-62.
42. Dorigo, W.; Wagner, W.; Hohensinn, R.; Hahn, S.; Paulik, C.; Xaver, A.; Gruber, A.; Drusch, M.; Mecklenburg, S.; Oevelen, P.v. The international soil moisture network: A data hosting facility for global in situ soil moisture measurements. *Hydrology and Earth System Sciences* **2011**, *15*, 1675-1698.

43. Mo, T.; Choudhury, B.; Schmugge, T.; Wang, J.; Jackson, T. A model for microwave emission from vegetation - covered fields. *Journal of Geophysical Research: Oceans* **1982**, *87*, 11229-11237.
44. Shi, J.; Jiang, L.; Zhang, L.; Chen, K.-S.; Wigneron, J.-P.; Chanzy, A. A parameterized multifrequency-polarization surface emission model. *IEEE Transactions on Geoscience and Remote Sensing* **2005**, *43*, 2831-2841.
45. Mladenova, I.; Jackson, T.; Njoku, E.; Bindlish, R.; Chan, S.; Cosh, M.; Holmes, T.; De Jeu, R.; Jones, L.; Kimball, J. Remote monitoring of soil moisture using passive microwave-based techniques—theoretical basis and overview of selected algorithms for amsr-e. *Remote sensing of environment* **2014**, *144*, 197-213.
46. Wagner, W.; Lemoine, G.; Rott, H. A method for estimating soil moisture from ers scatterometer and soil data. *Remote sensing of environment* **1999**, *70*, 191-207.
47. Brocca, L.; Tarpanelli, A.; Moramarco, T.; Melone, F.; Ratto, S.; Cauduro, M.; Ferraris, S.; Berni, N.; Ponziani, F.; Wagner, W. Soil moisture estimation in alpine catchments through modeling and satellite observations. *Vadose Zone Journal* **2013**, *12*.